

## Femtosecond laser pulse induced breakdown in dielectric thin films

J. Jasapara, A. V. V. Nampoothiri, and W. Rudolph\*

*Department of Physics and Astronomy, University of New Mexico, Albuquerque, New Mexico 87131*

D. Ristau and K. Starke

*Laser Zentrum Hannover e.V., D-30419 Hannover, Germany*

(Received 15 August 2000; published 9 January 2001)

Laser-induced breakdown of a high-quality mirror consisting of alternating  $\lambda/4$  layers of  $\text{Ta}_2\text{O}_5$  and  $\text{SiO}_2$  and a single 500-nm thin film of  $\text{Ta}_2\text{O}_5$  were studied with amplified and unamplified femtosecond pulses. The experimental data can be fitted with a model taking into account multiphoton absorption, impact ionization, and local intensity enhancements due to interference effects in the films. Incubation effects are observed when the coatings are damaged with multiple pulses from a femtosecond oscillator. The results indicate that state of the art, high-quality thin films show a damage behavior that is similar to bulk materials. Defects and impurities play a negligible role.

DOI: 10.1103/PhysRevB.63.045117

PACS number(s): 78.47.+p, 42.65.Re, 42.62.Cf, 79.20.Ds

### I. INTRODUCTION

The study of pulsed laser induced breakdown of thin films has been a subject of interest since the 1970s because of the need for optical coatings with high damage thresholds (see, for example, Ref. 1 and references therein). The breakdown of thin films induced by nanosecond and picosecond pulses was explained on the basis of a thermal model involving absorption by impurity centers and subsequent heat diffusion.<sup>2</sup> The threshold fluence was found to scale with the square root of the pulse duration  $\sqrt{\tau_p}$ . Recent work has concentrated on the damage of bulk dielectric materials with femtosecond (fs) pulses. The damage phenomena is found to be highly deterministic in this regime. With femtosecond pulses, energy is deposited into the material before any energy transfer to the lattice can occur. Hence the theory of bulk damage with long pulses<sup>3</sup> ( $>10$  ps) which is based on avalanche ionization, free-carrier absorption (inverse bremsstrahlung), and subsequent energy transfer to the lattice during the pulse is not applicable.

Dielectric breakdown in the femtosecond regime can be explained by the nonlinear excitation of electrons to the conduction band via processes such as avalanche ionization, tunneling ionization, and multiphoton absorption. When the conduction-band electron density reaches a critical plasma density of  $n_{cr} = 10^{21} \text{ cm}^{-3}$  (for  $\lambda \sim 800$  nm), the material absorbs strongly through the process of inverse bremsstrahlung resulting in ablation and permanent structural changes.<sup>4,5</sup> With recent advances in coating technology, thin films of very high quality can be produced. The breakdown of these films is expected to approach the limits determined by the intrinsic properties of the material rather than by impurities and defects.

In this paper we study femtosecond pulse induced breakdown of a single  $\text{Ta}_2\text{O}_5$  thin film on a fused silica substrate and of a broadband dielectric mirror consisting of alternating quarter-wave layers of  $\text{Ta}_2\text{O}_5$  and  $\text{SiO}_2$  ( $\lambda = 800$  nm). The layers were deposited by ion beam sputtering (IBS). Dielectric coatings produced by IBS are known for their nearly bulklike refractive indices, low optical losses, and high

breakdown thresholds, see for example Refs. 6 and 7.

A model that considers multiphoton absorption, impact ionization, and local intensity enhancements due to interference can be used to fit the experimental data. We compare breakdown induced by single pulses from an amplifier to breakdown with pulse trains from a femtosecond oscillator to investigate the effects of incubation.

### II. EXPERIMENT

The multiple shot experiments were performed with pulses from a femtosecond Ti:sapphire oscillator. This laser produced 10 fs pulses at 800 nm with an average power of 300 mW and 100-MHz repetition rate. The single shot experiments used pulses after amplification in a multipass 1-kHz repetition-rate amplifier. A schematic diagram of the experimental setup of the breakdown studies is shown in Fig. 1.

The high fluences required for inducing breakdown with pulses directly from the oscillator without amplification were obtained by tightly focusing the pulses with a high-numerical aperture ( $\text{NA} \sim 0.6$ ) microscope objective. The objective's radial dispersion properties were carefully characterized using spectral interferometry.<sup>8</sup> The information was used to precompensate the second- and third-order dispersion of the objective with a fused silica prism pair and a third-order dispersion mirror. The autocorrelation for the shortest pulse duration at the focus was measured to be  $\tau_p \sim 13$  fs with a two-photon photocurrent detector.<sup>9</sup> Translating one prism allowed us to tune the pulse duration continuously between 13 and 100 fs. The  $\omega_{1/e^2}$  spot size at the focus was measured to be  $600 \pm 50$  nm by scanning a metallic edge across the focus. The maximum pulse energy at the focus was  $\sim 1.5$  nJ.

The threshold pulse duration was measured as a function of the incident fluence. Figure 2 summarizes the experimental results obtained with the mirror. For every data point the pulse energy was kept constant while the pulse duration was decreased by translating one prism in the prechirper until breakdown occurred. The pulse fluence could be adjusted with a set of calibrated neutral density glass filters. The oc-

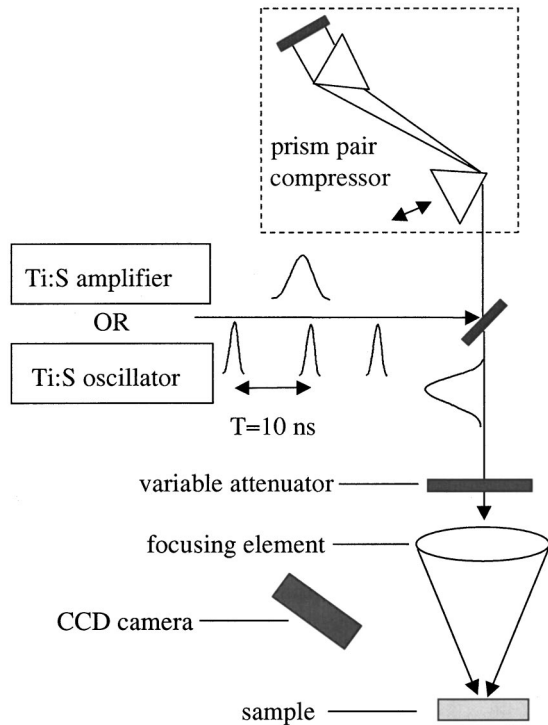


FIG. 1. Experimental setup for multiple shot studies with an oscillator and single shot studies with an amplifier. For single shot studies with the amplifier the focusing element is a  $f=50$  cm lens and the variable attenuator consists of a  $\lambda/2$  wave plate and polarizing beam splitter combination. For multiple pulse studies done with a pulse train from the oscillator, the focusing element is a  $100\times/0.6$  objective and the variable attenuator is a calibrated set of filters. The CCD camera was used in the single pulse experiments to monitor the scatter from the excited spot.

currence of damage was clearly visible as a change in the scattered light intensity and distribution on a screen behind the sample. Since the sample was illuminated with an infinite pulse train, rapid ablation occurred once the threshold pulse duration was reached. It should be noted that the breakdown threshold is extremely sharp. For pulse durations 1 fs longer

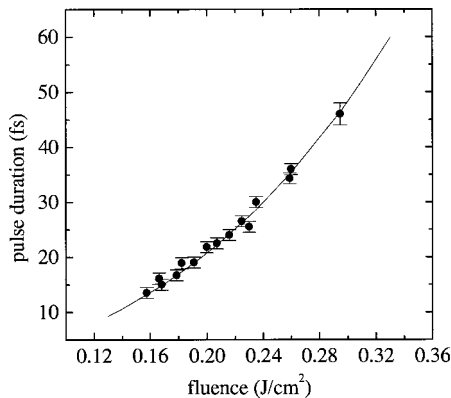


FIG. 2. Measured threshold pulse duration as a function of the incident pulse fluence for multiple pulse studies done on the mirror with the oscillator. The solid line is a fit of the model described in the text.

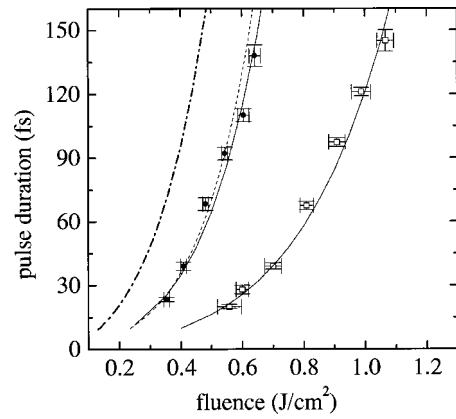


FIG. 3. Measured threshold pulse duration as a function of the incident pulse fluence for the high reflecting mirror (dots) and the 500-nm-thick single layer (hollow squares) under single shot illumination. The solid lines are a fit of the model described in the text. The dashed line is a curve with local intensity factor  $q=0.9$  and  $\alpha$  and  $\beta_3$  from the fit to the single layer. The dash-dot line is the fit to the multiple shot mirror data from Fig. 2 shown here again for comparison.

than the threshold, exposure of one and the same spot for several minutes did not lead to damage. Once the pulse duration was decreased breakdown with no visible time delay occurred. Also, the breakdown thresholds did not depend on how long the sample was preexposed to the pulse train at levels below the breakdown threshold.

In the single-pulse experiments, amplified pulses were focused onto the sample with a  $f=50$  cm lens. The  $\omega_{1/e^2}$  spot size at the focus measured by scanning a slit across the beam was found to be  $63 \pm 2 \mu m$ . The pulse energy could be tuned with a combination of a  $\lambda/2$  plate and a polarizing beam splitter. The energy of each pulse was monitored with a calibrated photodiode. The pulse duration was changed by tuning the prism pair compressor of the amplifier. We monitored the scattering of the amplified spontaneous emission (ASE) from the focal spot with a charge-coupled device (CCD) camera, although we did not resolve the illuminated site microscopically. Any pulse-induced changes of the scatter from the spot when illuminated by only the ASE (seed pulses from the oscillator were blocked) indicated damage. While similar to the detection by a photodiode, the two-dimensional detection of the scattering distribution proved to be more sensitive. We confirmed the accuracy of this method in a separate set of experiments where we observed the excited spot with a microscope. The sample was translated laterally after each shot to exclude pulse accumulation (incubation) effects.

Figure 3 shows the measurements done on the high reflecting mirror and the 500-nm  $Ta_2O_5$  single layer. For each data point the pulse duration was set with the compressor and the pulse energy was tuned with the  $\lambda/2$  plate to find the breakdown threshold.

### III. THEORY AND DISCUSSION

All breakdown experiments showed a very sharp and reproducible threshold behavior which is characteristic for

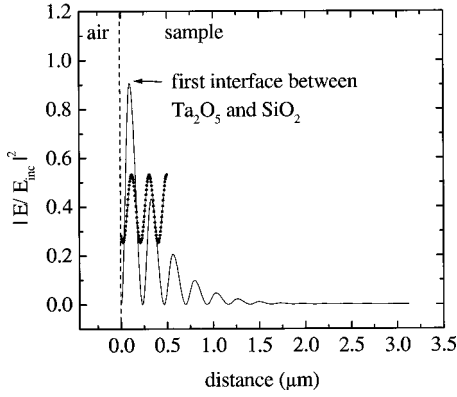


FIG. 4. Standing-wave intensity distribution in a high reflecting mirror consisting of 13 pairs of alternating  $\lambda/4$  layers of  $\text{Ta}_2\text{O}_5$  and  $\text{SiO}_2$  (solid line) and in the 500-nm single layer (dotted line). The mirror-coating sequence is  $S(HL)^{13}HA$ , where  $H$  is the high refractive index  $\text{Ta}_2\text{O}_5$  ( $n_H=2.1$ )  $\lambda/4$  layer,  $L$  is the low index  $\text{SiO}_2$  ( $n_L=1.45$ )  $\lambda/4$  layer,  $S$  is the substrate, and  $A$  stands for air.

damage of bulk materials induced by femtosecond pulses. Together with the observed dependence of the threshold fluence on the pulse duration, this suggests that the breakdown is due to intrinsic properties of the samples rather than due to impurities and defects.

Intrinsic breakdown of dielectrics can be explained by carrier generation due to high field ionization and impact ionization. If the so generated density of electrons in the conduction band reaches a critical value ( $n_{cr} \sim 10^{21} \text{ cm}^{-3}$ ) breakdown occurs.<sup>4,5</sup> The carrier generation is controlled by the local pulse intensity. Figure 4 compares the standing-wave intensity distribution in a single 500-nm film with that in the mirror structure. The mirror consists of a  $\text{Ta}_2\text{O}_5$  quarter-wave ( $\lambda = 800 \text{ nm}$ ) layer followed by 13 pairs of  $\text{SiO}_2/\text{Ta}_2\text{O}_5$  quarter-wave films and the fused silica substrate. From Fig. 4 one can expect that the breakdown fluence for the mirror is below that for the single layer. Also the mirror is most likely damaged at the first interface between  $\text{Ta}_2\text{O}_5$  and  $\text{SiO}_2$ . As will be explained below, the excitation is controlled by multiphoton absorption.  $\text{Ta}_2\text{O}_5$  ( $\text{SiO}_2$ ) has a band gap of  $\sim 4.1 \text{ eV}$  ( $9 \text{ eV}$ ). With our excitation wavelength ( $\sim 1.55 \text{ eV}$ ) we need a three- (six-) photon absorption to excite  $\text{Ta}_2\text{O}_5$  ( $\text{SiO}_2$ ). Thus breakdown is likely to occur first in the high-index  $\text{Ta}_2\text{O}_5$  layer. This was confirmed by experiments that yielded a breakdown threshold for  $\text{SiO}_2$  that is  $\sim 4$  times higher.

The rate of excitation of electrons to the conduction band in the presence of a strong electric field was derived by Keldysh.<sup>10</sup> The exact Keldysh expression simplifies to an expression for multiphoton absorption in the low-field, high-frequency limit, and to the tunneling expression in the low-frequency, high-electric-field limit. It turns out that for our range of excitation intensities and a broad range of reduced electron-hole masses,  $m_r > 0.2 m_e$  (where  $m_e$  is the free-electron mass), the exact Keldysh field ionization can be approximated by a multiphoton absorption process.

The other important mechanism for electron excitation is avalanche or impact ionization. The electrons excited to the conduction band by strong field ionization undergo oscillations

in the electric field. During these oscillations, they suffer momentum and energy changing collisions with the lattice. This process of inverse bremsstrahlung transfers energy to the electrons in the conduction band. When the kinetic energy of these electrons exceeds a certain critical value  $\epsilon_c$ , other electrons can be excited to the conduction band by collisions (impact ionization). The value of the critical energy is given by<sup>11</sup>

$$\epsilon_c \approx 1.5 \left( E_g + \frac{e^2 E_L^2}{4m_{er}\omega_L^2} \right), \quad (1)$$

where  $E_g$  is the band-gap energy,  $e$  is the electron charge,  $E_L$  is the electric field,  $\omega_L$  is the carrier frequency of the incident electric field, and  $m_{er} = (1/m_e^* + 1/m_{ev}^*)^{-1}$  is the reduced effective electron mass with  $m_e^*$  being the effective electron mass in the conduction band and  $m_{ev}^*$  being the effective electron mass in the valence band.

The flux-doubling model used by Stuart *et al.*<sup>4</sup> results in an impact-ionization rate that is proportional to the intensity. For it to hold the rate of impact ionization given by  $\epsilon_c P [(\epsilon - \epsilon_c)/\epsilon_c]^2$ , where  $P \approx 21 \text{ fs}^{-1}$  (see Ref. 11), must be much greater than the rate of Joule heating  $\sigma E_L^2$  where  $\sigma$  is the conductivity. This is equivalent to  $\sigma E_L^2 / P \epsilon_c \ll 1$  which is satisfied for our experimental conditions if we use  $\sigma = \sigma_{\max} = e^2 / (2m_e^* \omega_L)$  and assume  $m_e^* = m_{ev}^* = m_e$ . In the flux-doubling limit every conduction-band electron that reaches a kinetic energy of  $\epsilon_c$  immediately undergoes an ionizing collision leaving essentially no electrons with kinetic energy greater than  $\epsilon_c$  in the conduction band.

Using the approximations explained above, the rate of electron excitation to the conduction band can be written as

$$\frac{dn}{dt} = \alpha n(t) q I(t) + \beta_m [q I(t)]^m, \quad (2)$$

where  $\alpha$  is the impact-ionization coefficient,  $\beta_m$  is the  $m$ -photon absorption coefficient,  $I(t)$  is the incident pulse intensity, and  $q$  is a correction factor that takes into account interference effects in the coatings, cf. Fig. 4.

The solution to Eq. (2) for a pulse with a Gaussian temporal profile and  $m=3$  is given by

$$n(t) = e^{\gamma(t)} \left[ \left( \frac{4 \ln 2}{\pi} \right)^{3/2} \beta_3 \left( \frac{qF}{\tau_p} \right)^3 \int_{-\infty}^t e^{-3a^2 x^2 - \gamma(x)} dx + n_0 \right], \quad (3)$$

where  $\gamma(z) = (q\alpha F/2) [\text{erf}(az) + 1]$ ,  $a = 2\sqrt{\ln 2}/\tau_p$ ,  $n_0$  is the background electron density,  $\tau_p$  is the pulse duration, and  $F$  is the pulse fluence. The coefficients  $\alpha$  and  $\beta_3$  are unknown and are to be determined from the experimental data. To this end we fit the single pulse data of the 500-nm layer with  $n(\infty) = n_{cr}$ , where  $n(\infty)$  is determined from Eq. (3). The fit with the local intensity factor  $q=0.53$  is shown as a solid line in Fig. 3 and yields  $\alpha = 10 \pm 1.0 \text{ cm}^2 \text{ J}^{-1}$  and  $\beta_3 = 9.6 \pm 5 \times 10^{24} \text{ cm}^3 \text{ fs}^2 \text{ J}^{-3}$ . The error bars are due mainly to the uncertainty in the spot size measurements. A fit of the model to the mirror data with the local intensity factor  $q=0.9$  (cf. Fig. 4) gives  $\alpha = 9.7 \pm 1.0 \text{ cm}^2 \text{ J}^{-1}$  and  $\beta_3 = 7.2 \pm 1.5 \times 10^{24} \text{ cm}^3 \text{ fs}^2 \text{ J}^{-3}$ . This is in good agreement with the material pa-

rameters obtained from the study of the single layer. The main difference between the mirror and single-layer data is the different intensity enhancement factor  $q$ . To illustrate this we calculated the damage threshold using  $\alpha$  and  $\beta_3$  from the single layer and  $q$  from the mirror. The so obtained dashed line (cf. Fig. 3) agrees well with the experiment.

The fit values are insensitive to the value of  $n_0$  for  $n_0 \leq 10^{18} \text{ cm}^{-3}$ . The value of  $\alpha$  shows an order of magnitude agreement with those observed for other (bulk) dielectrics.<sup>4,5</sup> The fit value of the three-photon ionization coefficient  $\beta_3$  is typical for a three-photon band-gap material predicted by Keldysh's theory.<sup>10</sup> Under the assumption that  $m_r = m_e$ , a cubic fit to Keldysh's exact model predicts  $\beta_3 \approx 10^{25} \text{ cm}^3 \text{ fs}^2 \text{ J}^{-3}$  for a three-photon band-gap material.

A closer inspection of Eq. (3) with the values for  $\alpha$  and  $\beta_3$  obtained from the single shot experiments reveals that for short pulse durations ( $\sim 20$  fs) about 30% of the carriers are generated by multiphoton absorption. The contribution of avalanche ionization to the free-carrier generation increases with increasing pulse durations over the measured range, and reaches about 96% for 140-fs pulses. This is in accordance with the predictions<sup>4</sup> that multiphoton absorption plays a large role in the carrier generation in the short pulse limit and avalanche begins to play an increasingly dominant role as the pulse duration is increased.

Multiple pulse accumulation effects (incubation) are known to lower the breakdown threshold of materials.<sup>12,13</sup> This is also supported by our measurements with the pulse train from the femtosecond oscillator, cf. Fig. 2. On the other hand, the functional dependence of the threshold fluence on the pulse duration for the single and multiple pulse case is very similar. This suggests that the principal damage mechanisms are the same. The exact physical nature of the incubation is largely unknown and depends on the material. To discuss our multiple pulse data let us distinguish between two different accumulation effects—(i) accumulation of electrons in the conduction band governed by an effective relaxation time  $\tau$  and (ii) a continuous material modification during the excitation by the pulse train.

To include (i) we add a relaxation term  $n/\tau$  to Eq. (3). If we neglect the relaxation during the femtosecond pulse excitation we obtain an electron density after  $N$  pulses

$$n_N = e^{q\alpha F} \left[ \left( \frac{4 \ln 2}{\pi} \right)^{3/2} \beta_3 \left( \frac{qF}{\tau_p} \right)^3 \int_{-\infty}^{\infty} e^{-3a^2 x^2 - \gamma(x)} dx + n_0 \right] \times \frac{1 - p^N}{1 - p} - n_0 \frac{p - p^N}{1 - p}, \quad (4)$$

where  $p = \exp(q\alpha F - T/\tau)$  with  $T$  being the time period between two successive excitation pulses. To be consistent with our experiments  $p < 1$  must be satisfied. Otherwise breakdown would occur after a sufficiently large number  $N$  of pulses independent of the fluence. For  $p < 1$ , the limit  $n(N \rightarrow \infty) = n_\infty$  can be calculated from Eq. (4) and the result can be used to fit the data. Note that the limit  $p \rightarrow 0$  reproduces the single pulse result of Eq. (3). The quantity  $\tau$  is a phenomenological decay time that describes effects such as carrier recombination, trapping and diffusion. Recent experiments on other dielectric materials suggest that the value of

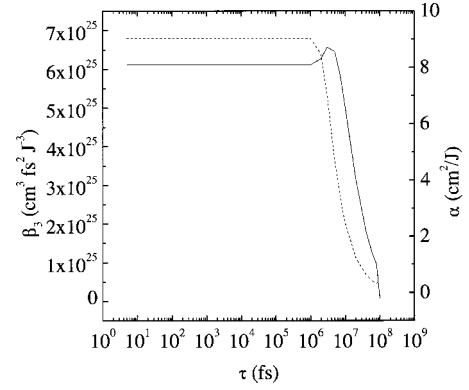


FIG. 5. Fit values of the three-photon ionization coefficient  $\beta_3$  (solid line) and avalanche coefficient  $\alpha$  (dashed line) as a function of the decay parameter  $\tau$ .

$\tau \leq 1$  ns.<sup>14</sup> Figure 5 shows the dependence of the fit results for the multiphoton absorption and impact-ionization coefficients as a function of  $\tau$  over a range for which  $p < 1$ .

For  $\tau < 1$  ns the fit is independent of  $\tau$  and yields  $\alpha = 9.0 \pm 2 \text{ cm}^2 \text{ J}^{-1}$  and  $\beta_3 = 6 \pm 3.5 \times 10^{25} \text{ cm}^3 \text{ fs}^2 \text{ J}^{-3}$ . Again the errors are due mainly to uncertainties in the spot size. While  $\alpha$  agrees with the value obtained from the single pulse experiment, the multiphoton coefficient is larger by about an order of magnitude. Hence incubation effects of type (i) alone cannot explain the experimental data. The nature of the observed incubation is such that it affects the generation of seed carriers on which the avalanche ionization acts. There is an effective increase in the multiphoton absorption coefficient  $\beta_3$  which can arise due to material modification [incubation processes of type (ii)] caused by, for example, stress development due to defect formation<sup>12</sup> or a change in the deformation potential.

#### IV. SUMMARY

Damage induced on  $\text{Ta}_2\text{O}_5$  single layers and a mirror consisting of  $\text{Ta}_2\text{O}_5/\text{SiO}_2$  pairs of quarter-wave layers was studied with single femtosecond pulses and pulse trains. The breakdown is highly deterministic and can be explained by multiphoton absorption and impact ionization when local intensity enhancements due to interference effects are taken into account. Under multiple pulse illumination the breakdown threshold is reduced. It can be explained by incubation mechanisms that increase the multiphoton absorption coefficient. Our data suggest that the breakdown is determined by intrinsic material properties rather than by impurities and defects. It is conceivable that the obtained values for the impact-ionization coefficient and multiphoton absorption coefficient can be used as figures of merit to predict laser pulse induced breakdown in high-quality dielectric thin films.

#### ACKNOWLEDGMENTS

This project was supported in part by NSF (Grant No. PHY-9601890) and NATO (Contract No. CRG-940652). The authors thank T. Apostolova, V.M. Kenkre, J. Krueger, J. McIver, and E. Welsch for valuable discussions.

\*Electronic address: wrudolph@unm.edu

<sup>1</sup>T.W. Walker, A.H. Guenther, and P.E. Nielsen, IEEE J. Quantum Electron. **QE-17**, 2041 (1981).

<sup>2</sup>M.R. Lange, J.K. McIver, and A.H. Guenther, Thin Solid Films **125**, 143 (1985).

<sup>3</sup>J.R. Bettis, R.A. House II, and A.H. Guenther, in *Laser Induced Damage in Optical Materials: 1976*, edited by A.J. Glass and A.H. Guenther, Natl. Bur. Stand. (U.S.) Spec. Publ. No. 462 (GPO, Washington, D.C., 1976), p. 338.

<sup>4</sup>B. Stuart, M. Feit, S. Herman, A. Rubenchik, B. Shore, and M. Perry, Phys. Rev. B **53**, 1749 (1996).

<sup>5</sup>M. Lenzner, J. Kruger, S. Sartania, Z. Cheng, C. Spielmann, G. Mourou, W. Kautek, and F. Krausz, Phys. Rev. Lett. **80**, 4076 (1998).

<sup>6</sup>D. Wei, Appl. Opt. **28**, 2813 (1989).

<sup>7</sup>R. Henking, Proc. SPIE **2428**, 281 (1994).

<sup>8</sup>J. Jasapara and W. Rudolph, Opt. Lett. **24**, 777 (1999).

<sup>9</sup>W. Rudolph, M. Sheikh-Bahae, A. Bernstein, and L. Lester, Opt. Lett. **22**, 313 (1997).

<sup>10</sup>L.V. Keldysh, Zh. Éksp. Teor. Fiz. **47**, 1945 (1964) [Sov. Phys. JETP **20**, 1307 (1965)].

<sup>11</sup>A. Kaiser, B. Rethfeld, M. Vicanek, and G. Simon, Phys. Rev. B **61**, 11 437 (2000).

<sup>12</sup>S.C. Jones, P. Braunlich, R.T. Casper, X.-A. Shen, and P. Kelly, Opt. Eng. (Bellingham) **28**, 1039 (1989).

<sup>13</sup>M. Lenzner, J. Kruger, W. Kautek, and F. Krausz, Appl. Phys. A: Mater. Sci. Process. **68**, 369 (1999).

<sup>14</sup>M. Li, S. Menon, J.P. Nibarger, and G.N. Gibson, Phys. Rev. Lett. **82**, 2394 (1999).